On *a-posteriori* pointwise error estimation using adjoint temperature and Lagrange remainder

A.K. Alekseev[a] and I. M. Navon[b]

a Department of Aerodynamics and Heat Transfer, RSC, ENERGIA, Korolev, Moscow Region 141070, Russian Federation

b Department of Mathematics and C.S.I.T., Florida State University, Tallahassee, FL 32306-4120, USA

Abstract

The calculation of the temperature error at a control point as a function of approximation error of a finite difference scheme is addressed. The local truncation error is determined by a Taylor series with the remainder in the Lagrange form. The contribution of the local error to the total pointwise error is estimated via an adjoint temperature. It is demonstrated that the results of numerical calculation of the temperature at an observation point may thus be refined via adjoint error correction and that a guaranteed error bound may be found.

Introduction. At present, there are many numerical methods enabling a very accurate calculation of temperature. Nevertheless, an estimation of the error of a concrete calculation is performed relatively rarely. From an historical perspective this is due to the huge computational burden of the numerical error calculation. The availability of increasing resources of computers has led to a significant raise in number of publications on this subject. In the finite-element analysis 'a posteriori' error analysis [1,23,24,28] is based on several approaches most of which are specific for this method. Nevertheless, an option based on the adjoint equations is applicable for any type of equations and is not limited by the framework of finite-element analysis. "A posteriori" error estimation is realized in [14-19] for Navier-Stokes and Euler equations. In these works the Galerkin method was used for the local errors estimation while the adjoint equations were used for calculation of their weights in a target

functional error. A similar approach was used in [9,10,12,25-27,33,34] for the refinement of practically useful functionals both by finite-element and finite-difference methods. The local error was estimated by interpolation, while its contribution was calculated using an adjoint problem. The information on the local error influence was used for grid refining. The Richardson extrapolation [21,29,30] is the most popular method for numerical error estimation in CFD. Unfortunately, it becomes complicated for schemes containing differences with a mixed order of accuracy and for problems with discontinuities. Many effects may change the nominal order of the grid convergence, for instance the presence of discontinuities. The simplest example is the reduction in convergence rate in presence of shocks. For schemes of third and fourth order of accuracy the reduction of the convergence rate was demonstrated in [5] for a compression wave. The works [6,7,31] confirm this effect. Certainly, a temperature field has no discontinuities, as a rule. Nevertheless, discontinuities in the gradient of temperature are rather common and potentially able to change the nominal convergence order. The spatial nonuniformity of the grid may also reduce the convergence rate ([35]). A correct use of Richardson extrapolation requires a set of grids to prove the monotonous convergence and to determine the real order of convergence for the considered solution. This may turn to be very expensive from a computer resources viewpoint.

In the present work we address the feasibility provided by adjoint equations for estimation of calculation error at a control point. We use the local truncation error determined by the Taylor series with the remainder in Lagrange form and an adjoint equation in continuous form. A simultaneous refinement and obtaining a guaranteed error bound are features specific to this approach. The refinement and the error bound are obtained on the same grid as that employed for the primal problem solution and require same computer time.

Numerical error estimation using the adjoint temperature

Let's consider the calculation of the temperature error at a checkpoint for finite-difference solution of the one dimensional thermal conduction equation.

$$C\rho\frac{\partial T}{\partial t}-\frac{\partial}{\partial x}\left(\lambda\frac{\partial T}{\partial x}\right)=0;\ (t,x)\in\Omega=(0<t<t_f;\ 0<x<X). \qquad (1)$$

Initial conditions: $T(0,x)=T_0(x);$ (2)

Boundary conditions $\frac{\partial T}{\partial x}\Big|_{x=0}=0;\ \frac{\partial T}{\partial x}\Big|_{x=X}=0.$ (3)

Consider a finite-difference approximation of the first order in time and second order in space.

$$C\rho\frac{T_k^n-T_k^{n-1}}{\tau}-\lambda\frac{T_{k+1}^n-2T_k^n+T_{k-1}^n}{h_k^2}=0; \qquad (4)$$

The simplicity of the scheme and the low order of approximation are deliberately chosen to illustrate the features of this approach with simplest mathematical treatment.

Let us expand the mesh function T_k^n in Taylor series and substitute to (4). Then equation (4) transforms to equation (5)

$$C\rho\frac{\partial T}{\partial t}-\frac{\partial}{\partial x}\left(\lambda\frac{\partial T}{\partial x}\right)+\delta T=0; \qquad (5)$$

Here $\delta T=\delta T_t+\delta T_x$ is a local truncation error engendered by Taylor series remainders. Thus, when solving the finite difference equation (4) we solve the differential approximation (5) instead of exact equation (1).

The error in the temperature calculation at a certain checkpoint $T_{est}=T(t_{est},x_{est})$ is determined by the sum of contributions of local truncation error with weights depending on the transfer of disturbances. For their determination let's denote the estimated temperature T_{est} by ε and express it as the functional.

$$T_{est} = \varepsilon = \iint\limits_{\Omega} T(t,x)\delta(t-t_{est})\delta(x-x_{est})dtdx \qquad (6)$$

The most efficient method for calculation of the functional variation is based on adjoint equations [22,4]. Let's use this approach here. For this purpose let's introduce a Lagrangian comprised of the estimated value and the weak statement of (1).

$$L = \iint\limits_{\Omega} T(t,x)\delta(t-t_{est})\delta(x-x_{est})dtdx +$$

$$+ \iint\limits_{\Omega} C\rho \frac{\partial T}{\partial t}\Psi(t,x)dtdx - \iint\limits_{\Omega} \frac{\partial}{\partial x}\left(\lambda \frac{\partial T}{\partial x}\right)\Psi(t,x)dtdx \qquad (7)$$

Local truncation errors represented in a form of the source $\delta T(t,x)$ disturb the temperature field. The corresponding problem for temperature disturbances assumes the form:

$$C\rho \frac{\partial \Delta T}{\partial t} - \frac{\partial}{\partial x}\left(\lambda \frac{\partial \Delta T}{\partial x}\right) + \delta T(t,x) = 0; \qquad (8)$$

Initial conditions: $\Delta T(0,x) = 0$ *;*

Boundary conditions $\frac{\partial \Delta T}{\partial x}\Big|_{x=0} = 0;\ \frac{\partial \Delta T}{\partial x}\Big|_{x=X} = 0;$ *(9)*

Problem (8) may be solved by using some part of Taylor expansion for sources $\delta T(t,x)$ estimation (as in [8]) that enables a correction of the target functional. Nevertheless, this is not sufficient for our purposes, since we are interested in the contribution of every grid cell to the total error and in obtaining a guaranteed error bound. So we continue the analysis and calculate the variation of the Lagrangian using equations (8-9).

$$\Delta L(\delta T) = \iint\limits_{\Omega} \Delta T\delta(t-t_{est})\delta(x-x_{est})dtdx + \iint\limits_{\Omega} \delta T\Psi\, dtdx +$$

$$+ \iint\limits_{\Omega} C\rho \frac{\partial \Delta T}{\partial t}\Psi\, dtdx - \iint\limits_{\Omega} \frac{\partial}{\partial x}\left(\lambda \frac{\partial \Delta T}{\partial x}\right)\Psi(t,x)dtdx; \qquad (10)$$

The integration of (10) by parts yields

$$\Delta L(\delta T) = \iint\limits_{\Omega} \Delta T\delta(t-t_{est})\delta(x-x_{est})dtdx + \iint\limits_{\Omega} \delta T\Psi\, dtdx -$$

$$-\iint\limits_{\Omega} C\rho\,\frac{\partial\Psi}{\partial t}\Delta T(t,x)\,dtdx + \int\limits_{x} C\rho\Psi(t,x)\Delta T dx\Big|_{t=0}^{t_f} -$$

$$-\iint\limits_{\Omega}\frac{\partial}{\partial x}\left(\lambda\frac{\partial\Psi}{\partial x}\right)\Delta T(t,x)dtdx - \int\limits_{t}\lambda\frac{\partial\Delta T}{\partial x}\Psi dt\Big|_{x=0}^{x=X} + \int\limits_{t}\lambda\frac{\partial\Psi}{\partial x}\Delta T dt\Big|_{x=0}^{x=X} \qquad (11)$$

We can express the variation of the Lagrangian via the source containing the local error of approximation.

$$\Delta L = \iint\limits_{\Omega}\delta T\Psi(t,x)dtdx \qquad (12)$$

Expression (12) is valid if other terms in (11) are equal to zero, i.e. on the solution of following ***adjoint problem***.

$$C\rho\,\frac{\partial\Psi}{\partial t} + \frac{\partial}{\partial x}\left(\lambda\,\frac{\partial\Psi}{\partial x}\right) - \delta(t - t_{est})\delta(x - x_{est}) = 0\,, \qquad (13)$$

$$\text{Boundary conditions:}\quad \frac{\partial\Psi}{\partial x}\Big|^{x=X} = 0,\ \frac{\partial\Psi}{\partial x}\Big|^{x=0} = 0\,, \qquad (14)$$

$$\text{Initial condition}\ \ \Psi(t_f, x) = 0; \qquad (15)$$

It is known, [22,4], that $\Delta\varepsilon(\delta T) = \Delta L(\delta T)$ on a solution of direct and adjoint problems. Thus we determine the variation of $T(t_{est}, x_{est})$.

$$\Delta\varepsilon = \Delta T_{est} = T_{est} - T_{exact} = \iint\limits_{\Omega}\delta T\Psi(t,x)dtdx \qquad (16)$$

Thus, the adjoint temperature enables us to calculate the variation of estimated parameter as a function of the truncation error. The adjoint problem is solved in the reverse temporal direction. It is determined by the direct problem and by a choice of a checkpoint. The present statement differs from adjoint equations used in Inverse Heat Transfer Problems [4] by the form of target functional and by the form of the source in (13). Usually, problem (13) is solved by a finite-difference method, so it also contains an error $\Psi(t,x) = \Psi_{exact}(t,x) + \Delta\Psi(t,x)$. So, the error of the temperature at a checkpoint may be divided into two parts

$$\Delta\varepsilon = \Delta T_{est} = \iint\limits_{\Omega} \delta T \Psi_{exact}(t,x)dtdx + \iint\limits_{\Omega} \delta T \Delta\Psi(t,x)dtdx \qquad (17)$$

Several works [9,10,12,25-27,33,34] consider a minimization of the second part of expression (17) as a means for diminishing the inherent error.

The calculation of error caused by temporal approximation. The error ΔT_{est} is determined as a function of the adjoint temperature and a truncation error. Let's expand the mesh function T_k^n using the Taylor series with the Lagrange remainder and substitute it to finite differences (3). For the temporal part of truncation error we obtain

$$\frac{T_k^n - T_k^{n-1}}{\tau} = \frac{\partial T}{\partial t} - \frac{1}{2}\left(\tau \frac{\partial^2 T(t_n - \alpha_k^n \tau, x_k)}{\partial t^2}\right) \qquad (18)$$

Parameters $\alpha_k^n \in (0,1)$ are unknown.

The last term in (18) determines δT_t **,** while corresponding error ΔT_{est} has the form

$$\Delta\varepsilon(\delta T_t) = -\frac{C\rho}{2}\int\limits_{\Omega}\left(\tau \frac{\partial^2 T(t_n - \alpha_k^n \tau, x_k)}{\partial t^2}\right)\Psi\, dxdt \qquad (19)$$

Further discussion is significantly devoted to the calculation of magnitude and bounds of expression (19) and its analogues. Let's present (19) in a discrete form, for example:

$$\Delta\varepsilon(\delta T_t) = -\frac{C\rho}{2}\sum_{k=1,n=2}^{Nx,Nt}\left(\tau \frac{\partial^2 T(t_n - \alpha_k^n \tau, x_k)}{\partial t^2}\right)\Psi_k^n h_k \tau \qquad (20)$$

Equation (20) may be expanded in series over $\alpha_k^n \tau$,

$$\Delta\varepsilon(\delta T_t) = -\frac{C\rho}{2}\sum_{k=1,n=2}^{Nx,Nt}\left(\tau \frac{\partial^2 T(t_n, x_k)}{\partial t^2} - \tau\alpha_k^n \tau \frac{\partial^3 T(t_n, x_k)}{\partial t^3} + \frac{(\alpha_k^n \tau)^2}{2}\tau \frac{\partial^4 T(t_n, x_k)}{\partial t^4} - \ldots\right)\Psi_k^n h_k \tau \qquad (21)$$

The first part of sum (21) may be used for correction of the functional

$$\Delta T_t^{corr} = -\frac{C\rho}{2}\sum_{k=1,n=2}^{Nx,Nt}\frac{\partial^2 T(t_n, x_k)}{\partial t^2}\Psi_k^n h_k \tau^2 \qquad (22)$$

The second part of (21) contains unknown parameters $\alpha_k^n \in (0,1)$. If only first order term over $\alpha_k^n \tau$ is retained in (21) an upper bound may be obtained

$$\frac{C\rho}{2}\sum_{k=1,n=2}^{Nx,Nt}\alpha_k^n\tau^3\frac{\partial^3 T(t_n,x_k)}{\partial t^3}\Psi_k^n h_k \le \frac{C\rho}{2}\sum_{k=1,n=2}^{Nx,Nt}\left|h_k\tau^3\frac{\partial^3 T(t_n,x_k)}{\partial t^3}\Psi_k^n\right| = \Delta T_{t,1}^{\sup} \qquad (23)$$

Using this value we can determine the upper bound of the functional error (after refining):

$$\left|T - \Delta T_t^{corr} - T_{exact}\right| < \Delta T_{t,1}^{\sup} \qquad (24)$$

Expression (23) is the Holder inequality applied to the scalar product $(\alpha_k^n\Theta_k^n)$,

$\sum_{k=1,n=2}^{Nx,Nt}\alpha_k^n\Theta_k^n = (\alpha_k^n\Theta_k^n) \le \left\|\alpha_k^n\right\|_p\left\|\Theta_k^n\right\|_q$, $\quad \frac{1}{p}+\frac{1}{q}=1$. $\quad \left\|\alpha\right\|_p = \left(\left|\alpha_1\right|^p + \left|\alpha_2\right|^p + ...\left|\alpha_N\right|^p\right)^{1/p}$,

$\left\|\alpha\right\|_\infty = \max\left(\left|\alpha_i\right|\right)$. This approach enables us to obtain estimations for other terms in (21) also. For example, the estimation of the second (over $\alpha_k^n\tau$) order term has the form

$$-\frac{C\rho}{2}\sum_{k=1,n=2}^{Nx,Nt}\left(\frac{(\alpha_k^n\tau)^2}{2}\tau\frac{\partial^4 T(t_n,x_k)}{\partial t^4}\right)\psi_k^n h_k\tau < \frac{C\rho}{2}\sum_{k=1,n=2}^{Nx,Nt}\left|\frac{1}{2}\tau^4 h_k\psi_k^n\frac{\partial^4 T(t_n,x_k)}{\partial t^4}\right| = \Delta T_{t,2}^{\sup} \qquad (25)$$

The estimation of the error taking into account of the second term may be written as

$$\left|T - \Delta T_t^{corr} - T_{exact}\right| < \Delta T_{t,1}^{\sup} + \Delta T_{t,2}^{\sup} \qquad (26)$$

On a sufficiently smooth solution, every next term of series $\Delta T_{t,s}^{\sup}$ has an order that is greater by unit. For an infinitely smooth solution expression (26) may be stated as $\left|T - \Delta T_t^{corr} - T_{exact}\right| < \sum_{s=1}^{\infty}\Delta T_{t,s}^{\sup}$. If all derivatives are bounded, this series converges $\sum_{k=1,n=2}^{Nx,Nt}\left|\frac{(\alpha_k^n\tau)^s}{s!}\frac{\partial^{s+2}T(t_n,x_k)}{\partial t^{s+2}}\Psi_k^n h_k\tau^2\right| < C\tau\frac{\tau^s}{s!}$, nevertheless, this does not guarantee the estimation to be small enough to have a practical significance.

The applicability of such estimates may be complicated by discontinuities of the derivatives. Let's consider this problem at the heuristic level. For this purpose let us write (21) in more detail.

$$\Delta\varepsilon(\delta T) = -\frac{C\rho}{2}\sum_{k=1,n=2}^{Nx,Nt}\left(\tau\frac{\partial^2 T(t_n,x_k)}{\partial t^2} - \tau\alpha_k^n\tau\frac{\partial^3 T(t_n,x_k)}{\partial t^3} + ... + \frac{(-\alpha_k^n\tau)^s}{s!}\tau\frac{\partial^{s+2}T(t_n,x_k)}{\partial t^{s+2}} + ...\right)\Psi_k^n h_k\tau \qquad (27)$$

Let *m* be the number of bounded derivatives (derivatives of the order *m* and higher may have a finite number of jump discontinuities), *p* is the order of the approximated derivative, *j* is the formal order of accuracy of a finite-difference scheme. Let's approximate derivatives by the finite differences $\frac{DT(t,x)}{Dt}$. The limit $\lim_{\tau\to 0}\sum_{\Omega}\left(\tau^j \frac{D^{p+j}T(t,x)}{Dt^{p+j}}\right)h\Psi\tau$ corresponds to the first term (27). Consider its asymptotic form. The derivative of order *m+1* has an asymptotic $(T_+^{(m)} - T_-^{(m)})/\tau \sim \Delta/\tau$ for the jump discontinuity**,** while the derivative of order *m+2* has the asymptotic $(\Delta/\tau - 0/\tau)/\tau \sim \Delta/\tau^2$**,** correspondingly the derivative of the order $p + j$ has the asymptotic $\frac{\Delta}{\tau^{p+j-m}}$**.** Thus $\lim_{\tau\to 0}\left(\tau^j \frac{D^{p+j}T(t,x)}{Dt^{p+j}}\right) \sim \lim_{\tau\to 0}\left(\tau^j \frac{\Delta}{\tau^{p+j-m}}\right)$**.** There are a limited number of nodes that participate in the summation in the vicinity of discontinuity, so the multiplier τ (appearing during summation) should be taken into account, yielding $\sum_{k=1,n=n_r-n_s}^{k=Nx,n=n_r+n_s}\left(\tau^j \frac{D^{p+j}T(t,x)}{Dt^{p+j}}\right)h\Psi\tau \sim \tau^{m-p+1}$.

Thus, the terms of *j-th* formal order of accuracy contain a component of *j-th* order (appearing due to integration over the smooth part of the solution) and a component having the order $i = m - p + 1$ (engendered by the jump discontinuity of the $m - th$ order derivative**).** So, the order of convergence depends on the solution and may asymptotically tend to a minimal order $i = m - p + 1$ as grid size decreases. This is also relevant to other terms in (27).

If we have a sufficient number of smooth derivatives, we can restrict the number of terms in expansion (21) in order to avoid using derivatives of order higher than *m*. Let *m=3,* then in our case ($m = j + 2$ **)**

$$\Delta\varepsilon(\delta T) = -\frac{C\rho}{2}\sum_{k=1,n=2}^{Nx,Nt}\left(\tau\frac{\partial^2 T(t_n,x_k)}{\partial t^2} - \tau\alpha_k^n\tau\frac{\partial^3 T(t_n-\eta_k^n\alpha_k^n\tau,x_k)}{\partial t^3}\right)\Psi_k^n h_k\tau \qquad (28)$$

The derivatives in (28) are related to some points within the interval $\eta_k^n \in (0,1)$**.** Correspondingly, the estimation of error bound has the form

$$\Delta T_{t,1}^{\sup} = \frac{C\rho}{2} \sum_{k=1,n=2}^{Nx,Nt} \left| \tau^2 \frac{\partial^3 T(t_n - \eta_k^n \alpha_k^n \tau, x_k)}{\partial t^3} \Psi_k^n \right| h_k \tau \qquad (29)$$

If the third derivative is bounded, the deviation of (29) from (23) $\left(\frac{C\rho}{2} \sum_{k=1,n=2}^{Nx,Nt} \left| \tau^2 \frac{\partial^3 T(t_n, x_k)}{\partial t^3} \Psi_k^n \right| h_k \tau \right)$ is not large. Let *m=2,* the third derivative is not bounded and the deviation of (29) from (23) may be large. In this case we should consequently estimate terms of series (27) (having the same order on τ) in the hope that the presence of the factorial *s!* in (27) would enable us to stop summing at a certain term.

Later we will consider in numerical tests the influence of discontinuities on the error, for example that of the temperature spatial derivative.

The calculation of error caused by spatial approximation. Similarly to previous treatment we use Taylor series with a Lagrange remainder in order to determine the discretization error of the spatial derivative. ($\beta_k^n \in (0,1)$, $\gamma_k^n \in (0,1)$ are unknown).

$$T_{k+1}^n = T_k^n + h_k \frac{\partial T}{\partial x} + \frac{1}{2} h_k^2 \frac{\partial^2 T}{\partial x^2} + \frac{1}{6} h_k^3 \frac{\partial^3 T}{\partial x^3} + \frac{1}{24} h_k^4 \left(\frac{\partial^4 u(t_n, x_k + \beta_k^n h_k)}{\partial x^4} \right) = 0$$

$$T_{k-1}^n = T_k^n - h_k \frac{\partial T}{\partial x} + \frac{1}{2} h_k^2 \frac{\partial^2 T}{\partial x^2} - \frac{1}{6} h_k^3 \frac{\partial^3 T}{\partial x^3} + \frac{1}{24} h_k^4 \left(\frac{\partial^4 u(t_n, x_k - \gamma_k^n h_k)}{\partial x^4} \right) = 0$$

Then

$$\frac{T_{k+1}^n - 2T_k^n + T_{k-1}^n}{h_k^2} = \frac{\partial^2 T}{\partial x^2} + \frac{1}{24} h_k^2 \left(\frac{\partial^4 T(t_n, x_k + \beta_k^n h)}{\partial x^4} + \frac{\partial^4 T(t_n, x_k - \gamma_k^n h)}{\partial x^4} \right) \qquad (30)$$

The computational error related to a truncation error of spatial approximation has the form

$$\Delta\varepsilon(\delta T_x) = -\int_{\Omega} \frac{\lambda}{24} h_k^2 \left(\frac{\partial^4 T(t_n, x_k + \beta_k^n h)}{\partial x^4} + \frac{\partial^4 T(t_n, x_k - \gamma_k^n h)}{\partial x^4} \right) \Psi \, dx dt \qquad (31)$$

Its discrete form

$$\Delta\varepsilon(\delta T_x) = -\frac{\lambda}{24} \sum_{k=1,n=1}^{Nx,Nt} h_k^2 \left(\frac{\partial^4 T(t_n, x_k + \beta_k^n h)}{\partial x^4} + \frac{\partial^4 T(t_n, x_k - \gamma_k^n h)}{\partial x^4} \right) \Psi_k^n h_k \tau$$

in the first order in $\beta_k^n h, \gamma_k^n h$ may me formulated as

$$\Delta\varepsilon(\delta T_x) = -\frac{\lambda}{12}\sum_{k=1,n=2}^{Nx,Nt} h_k^3 \frac{\partial^4 T(t_n, x_k)}{\partial x^4}\Psi_k^n \tau -$$

$$-\frac{\lambda}{24}\sum_{k=1,n=2}^{Nx,Nt} h_k^3\left(\frac{\partial^5 T(t_n, x_k)}{\partial x^5}\beta_k^n - \frac{\partial^5 T(t_n, x_k)}{\partial x^5}\gamma_k^n\right)\Psi_k^n h_k \tau \qquad (32)$$

The first part of this sum can be used for a correction

$$\Delta T_x^{corr} = -\frac{\lambda}{12}\sum_{k=1,n=1}^{Nx,Nt} h_k^3 \frac{\partial^4 T(t_n, x_k)}{\partial x^4}\Psi_k^n \tau \qquad (33)$$

The inherent error is engendered by the second part terms. We can obtain a bound for it by assuming $\beta_k^n - \gamma_k^n = 1$.

$$\frac{\lambda}{24}\sum_{k=1,n=2}^{Nx,Nt} h_k^3\left(\frac{\partial^5 T(t_n, x_k)}{\partial x^5}\beta_k^n - \frac{\partial^5 T(t_n, x_k)}{\partial x^5}\gamma_k^n\right)\Psi_k^n h_k \tau < \Delta T_{x,1}^{\sup} = \frac{\lambda}{24}\sum_{k=1,n=2}^{Nx,Nt} h_k^4\left|\frac{\partial^5 T(t_n, x_k)}{\partial x^5}\Psi_k^n\right|\tau \qquad (34)$$

The density in (34) represents the contribution of every cell to the total error, so it may serve for the design of a grid that minimizes it.

Numerical tests. The error is calculated for the temperature field evolution engendered by a pointwise heat source (t_0, ξ -is the initial time and the coordinate of the point source).

$$T_{an}(t, x) = \frac{Q}{2\sqrt{\pi\lambda/(C\rho)(t - t_0)}}\exp\left(-\frac{(x-\xi)^2}{4\lambda/(C\rho)(t - t_0)}\right) \qquad (35)$$

We use the data $f_k = T_0(x_k)$ calculated by (35) as the initial data when solving (4). The length X of spatial interval is chosen so as to provide a negligible effect of the boundary condition compared with the effect of approximation. The round-off errors were estimated by comparing calculation with single and double precision, and the difference was negligible. We should ascertain that the error $\iint_\Omega \delta T \Delta\Psi(t, x) dt dx$ engendered by adjoint equation approximation is sufficiently small. For calculation of $\Delta\Psi(t, x)$ the following equation was

used

$$C\rho\frac{\partial\Delta\Psi}{\partial t}+\frac{\partial}{\partial x}\left(\lambda\frac{\partial\Delta\Psi}{\partial x}\right)+\delta\Psi_t(t,x)+\delta\Psi_x(t,x)=0; \qquad (36)$$

(second order adjoint equation [36,2]). Corresponding error of functional has the form: $\Delta\varepsilon(\delta T)=-\frac{C\rho}{2}\sum_{k=1,n=2}^{Nx,Nt}\left(\tau\frac{\partial^2 T(t_n,x_k)}{\partial t^2}\right)\Delta\Psi_k^n h_k\tau$. As expected, the computations demonstrated that the part of error (17) related to the adjoint temperature error is significantly smaller than the main value (connected with the adjoint temperature itself).

An implicit method (implemented by the Thomas algorithm) was used for solution both of the heat transfer equation and the adjoint equations of first and second orders. The spatial grid consisted of 100–1000 nodes, the temporal integration contained 100-10000 steps. Thermal conductivity was $\lambda=10^{-4}$ kW/(m·K), volume heat capacity was equal to $C\rho=500$ kJ/(m^3·K). The initial and final temperature distributions are presented in Figure 1 together with zones of error estimation.

The temperature errors were calculated via adjoint equations and compared with the deviation of the numerical solution from analytical one (35).

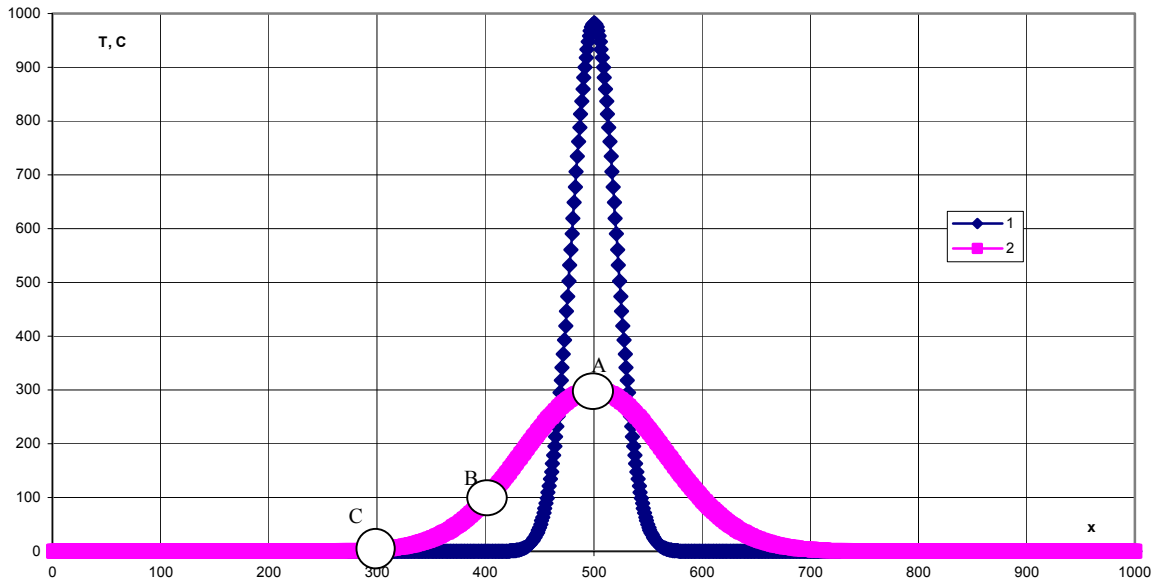

Fig 1 Initial and final temperature distribution. 1 - Initial temperature, 2- Final temperature

Isolines of temperature and adjoint temperature are presented in Figures 2 and 3 for one of computed variants.

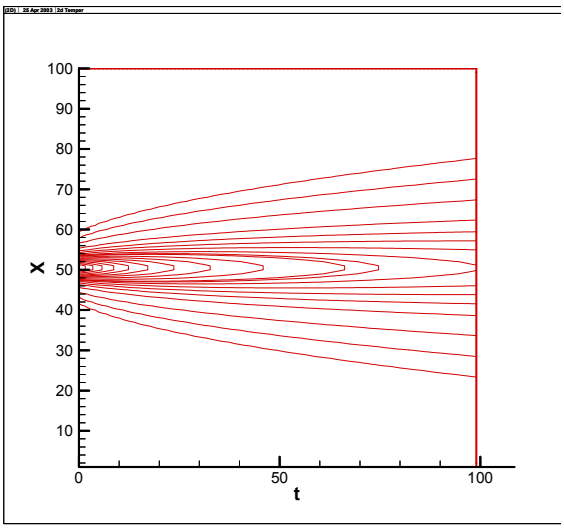

Fig. 2. Temperature isolines

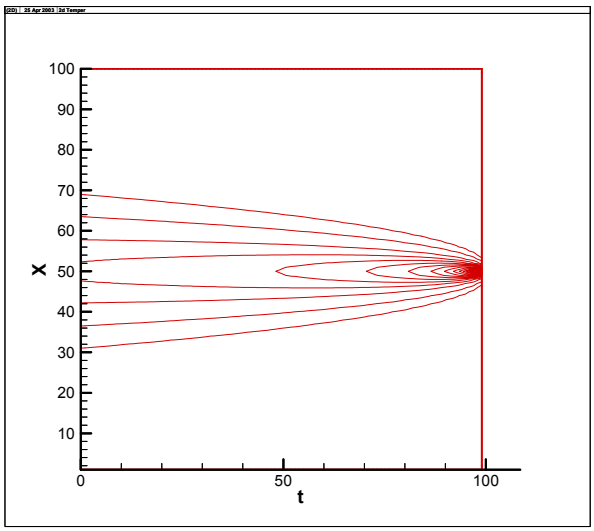

Fig. 3. Adjoint temperature isolines

As previously mentioned, the adjoint temperature may be considered as a weight coefficient determining the contribution of the truncation error to the error of estimated parameter. Thus, Figure 3 describes the relative weights of the truncation error contribution to the temperature at the estimated point.

The error of temperature calculation caused by the time discretization.

Estimates of temperature calculation error depending a time step are presented in Table 1 (central point at the final moment). The spatial step is chosen to be enough small

(h=0.0001 m) so as to provide a small impact of the spatial discretization error in comparison with the temporal one. The error $\int \delta T \Delta\Psi$ caused by adjoint temperature approximation was calculated using equation (36) and was significantly smaller then the temporal one.

Table 1

τ , sec	$T - T_{an}$	ΔT_t^{corr} (23)	$T_t^{corr} - T_{an}$	ΔT^{err}	$\Delta T_{t,1}^{\sup}$ (25)	ΔT_x^{corr} (33)	$\Delta T_{x,1}^{\sup}$ (34)	$\int \delta T \Delta\Psi$
0.1	0.1007	0.09301	0.0077	$-5.0\cdot10^{-5}$	0.0113	$7.75\cdot10^{-3}$	$5.4\cdot10^{-3}$	$-8.\cdot10^{-5}$
0.2	0.1938	0.1856	0.0082	$4.0\cdot10^{-4}$	0.0429	$7.78\cdot10^{-3}$	$5.41\cdot10^{-3}$	$-3.\cdot10^{-4}$
0.4	0.3790	0.3699	0.0091	$1.3\cdot10^{-3}$	0.156	$7.8\cdot10^{-3}$	$5.4\cdot10^{-3}$	$-1.\cdot10^{-3}$
0.8	0.7400	0.7341	0.0059	$-1.9\cdot10^{-3}$	0.524	$7.84\cdot10^{-3}$	$5.4\cdot10^{-3}$	$-5.\cdot10^{-3}$
1	0.9189	0.9141	0.0048	$-3.0\cdot10^{-3}$	0.76	$7.86\cdot10^{-3}$	$5.36\cdot10^{-3}$	$-8.\cdot10^{-3}$
2	1.7904	1.7932	-0.0028	$-1.0\cdot10^{-2}$	2.15	$7.97\cdot10^{-3}$	$5.32\cdot10^{-3}$	$-3.\cdot10^{-2}$

Here $T - T_{an}$ is the difference between the numerical and analytical calculations, $T^{corr} = T - \Delta T_t^{corr} - \Delta T_x^{corr}$ is the refined solution, $\Delta T_{t,1}^{\sup}$ is the upper bound of error (25), $\Delta T_{x,1}^{\sup}$ is the upper bound of error (34). $\Delta T^{err} = T - \Delta T_t^{corr} - \Delta T_x^{corr} - T_{an}$ is the deviation of refined solution from the analytical one. The linear character of error (23) variation depending on the time step should be emphasized. The error of calculation is practically eliminated by correction using ΔT_t^{corr} and ΔT_x^{corr}, the remaining part is in the range of bound $\Delta T_{t,1}^{\sup}$. The error caused by the adjoint equation approximation $\int \delta T \Delta\Psi$ is small enough and close to ΔT^{err}, its quadratic dependence on a temporal step may be noted.

Figures 4,5 and 6 illustrate a comparison between analytic, finite-difference and corrected finite-difference solutions and the error bounds (h=0.0001 m, τ=1.0 sec) in different zones (Fig 1).

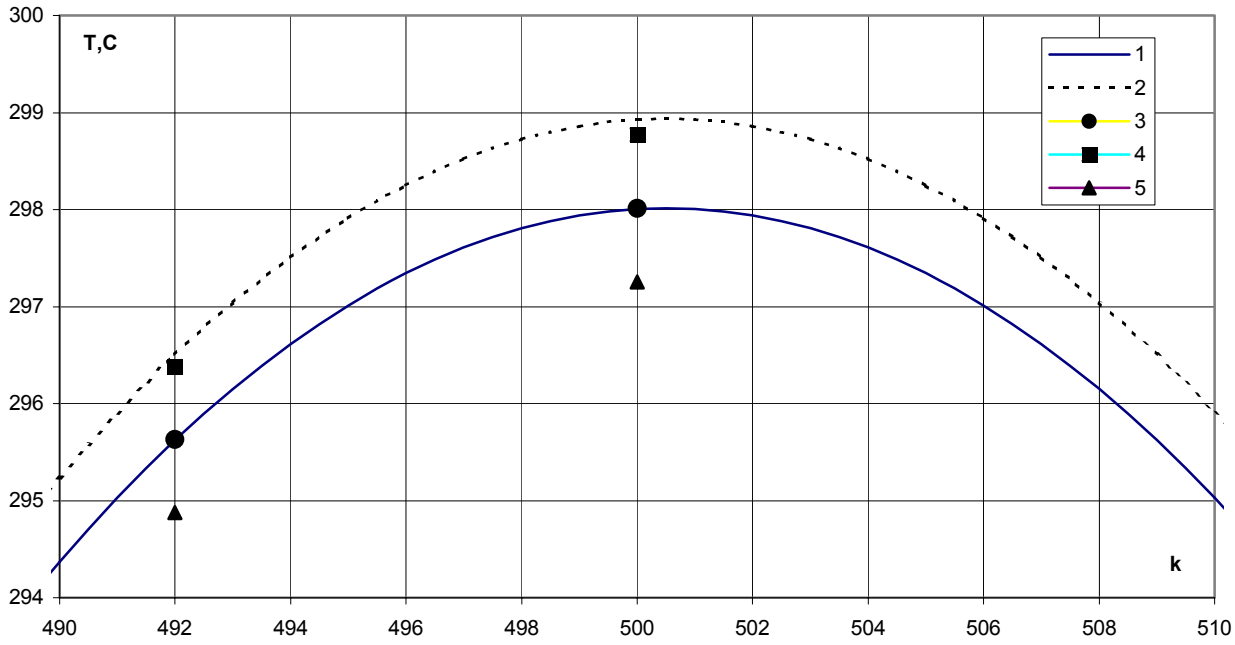

Fig. 4. The comparison of numerical and analytical solutions in zone A (Fig. 1). 1- analytical, 2-numerical, 3-refined solution, 4- upper bound, 5- lower bound

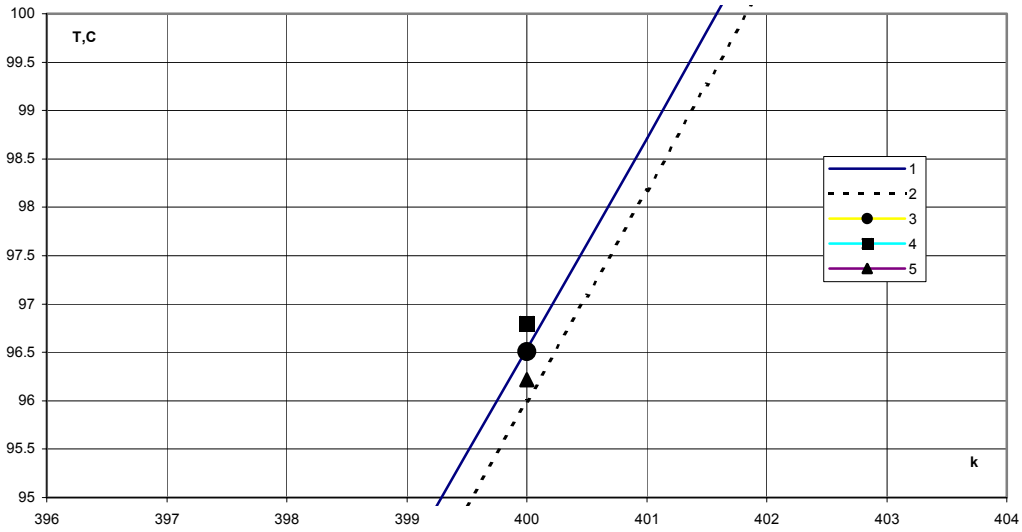

Fig. 5. The comparison of numerical and analytical solutions in zone B. 1- analytical, 2-numerical, 3- refined solution, 4- upper bound, 5 lower bound

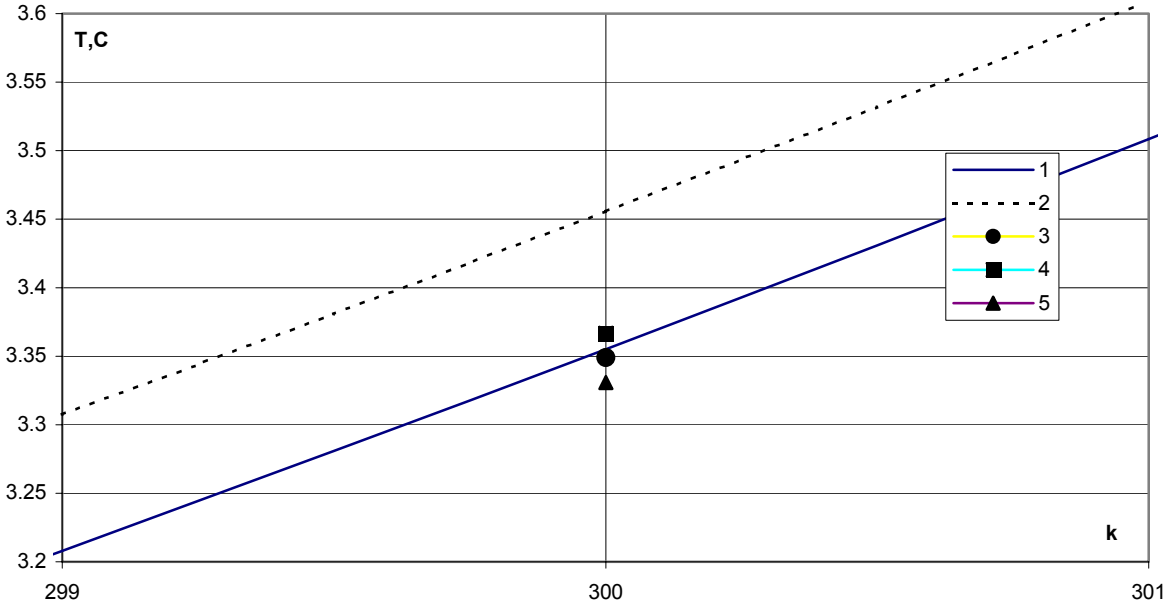

Fig. 6. The comparison of numerical and analytical solutions in zone C. 1- analytical, 2-numerical, 3- refined solution, 4- upper bound, 5 lower bound

The error of temperature calculation engendered by the spatial discretization.

Let's consider the error caused by the spatial approximation. In order to determine this error, let's provide a small contribution of truncation error of the temporal approximation. With this purpose a second order time differencing scheme was used.

$$C\rho\frac{T_k^{n-1/2}-T_k^{n-1}}{\tau}-\frac{1}{2}\lambda\frac{T_{k+1}^{n-1}-2T_k^{n-1}+T_{k-1}^{n-1}}{h_k^2}=0;$$

$$C\rho\frac{T_k^{n}-T_k^{n-1/2}}{\tau}-\frac{1}{2}\lambda\frac{T_{k+1}^{n}-2T_k^{n}+T_{k-1}^{n}}{h_k^2}=0; \qquad (37)$$

It may be demonstrated similarly to previous treatments that the error caused by the temporal approximation is of second order in τ.

$$\Delta\varepsilon(\delta T)=-\frac{C\rho}{12}\sum_{k=1,n=2}^{Nx,Nt}\frac{\partial^3 T(t_n,x_k)}{\partial t^3}\Psi_k^n h_k\tau^3 \qquad (38)$$

A bound of the inherent error caused by temporal step is:

$$\Delta T_t^{\sup} = \Delta\varepsilon(\delta T) = \frac{C\rho}{4}\sum_{k=1,n=2}^{Nx,Nt}\left|\frac{\partial^4 T(t_n,x_k)}{\partial t^4}\Psi_k^n\right|h_k\tau^4 \qquad (39)$$

The error caused by the spatial approximation preserves its previous form (33,34).

Numerical tests demonstrated that the error caused by the time step (38) was not greater than $2\cdot 10^{-5}$ and was significantly smaller than the error caused by the spatial approximation. The error caused by the adjoint equation approximation $\iint_{\Omega}\delta T\Delta\Psi(x,t)dtdx$ was still smaller by several orders of magnitude. The temperature error estimations as a function of the spatial step size are presented in Table 2 (for central point at the final time).

Table 2. **Temperature error estimations depending on the spatial step.**

H, m	$T - T_{an}$, K	ΔT_x^{corr} (33)	$T_x^{corr} - T_{an}$	$\Delta T_x^{\sup}$ (34)
0.002	3.0607	2.719	0.341	6.3
0.001	0.772345	0.751934	0.0204	1.86
0.0008	0.494818	0.48683	0.0080	1.08
0.0004	0.123853	0.123579	$2.74 \cdot 10^{-4}$	0.163
0.0002	0.030948	0.031011	$6.3 \cdot 10^{-6}$	$2.1 \cdot 10^{-2}$
0.0001	0.007711	0.007760	$4.9 \cdot 10^{-5}$	$2.7 \cdot 10^{-3}$

In Table 2 $T_x^{corr} = T - \Delta T_x^{corr}$ is the finite difference solution refined using adjoint temperature. The comparison of deviations of solution and refined solution from analytical one ($T - T_{an}$ and $T_x^{corr} - T_{an}$) demonstrates that the refinement by ΔT_x^{corr} (33) enables us to eliminate a significant part of the error. Comparison of the remaining error $T_x^{corr} - T_{an}$ and $\Delta T_x^{\sup}$ demonstrates a reliable satisfaction of the bound (34). The quadratic character of ΔT_x^{corr} and the third order of $\Delta T_x^{\sup}$ should be noted. The convergence rate of ΔT_x^{corr} and $\Delta T_x^{\sup}$ demonstrates that the discontinuities of high order derivatives for equation (1) under initial conditions (35) and boundary conditions (2) did not engender any visible effect (they are located in zones of small Ψ).

Fig. 7 demonstrates the initial and final temperature distributions (*h=0.001 m*, τ=0.1 sec). Fig. 8 and 9 provide a comparison of the analytical, finite-difference and refined solutions and the error bound at different points (zones A and B, Fig 7). The spatial step is chosen large enough for visibility and for suppression of other errors. Naturally, the error is smaller for finer grid (Table 2).

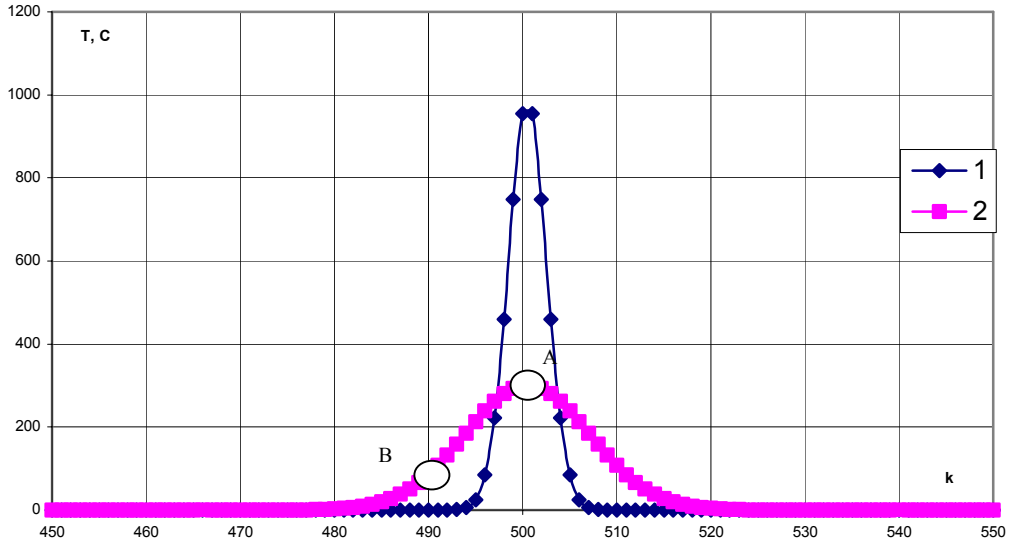

Fig. 7. Initial and final temperature distribution. 1- Initial temperature, 2- Final temperature

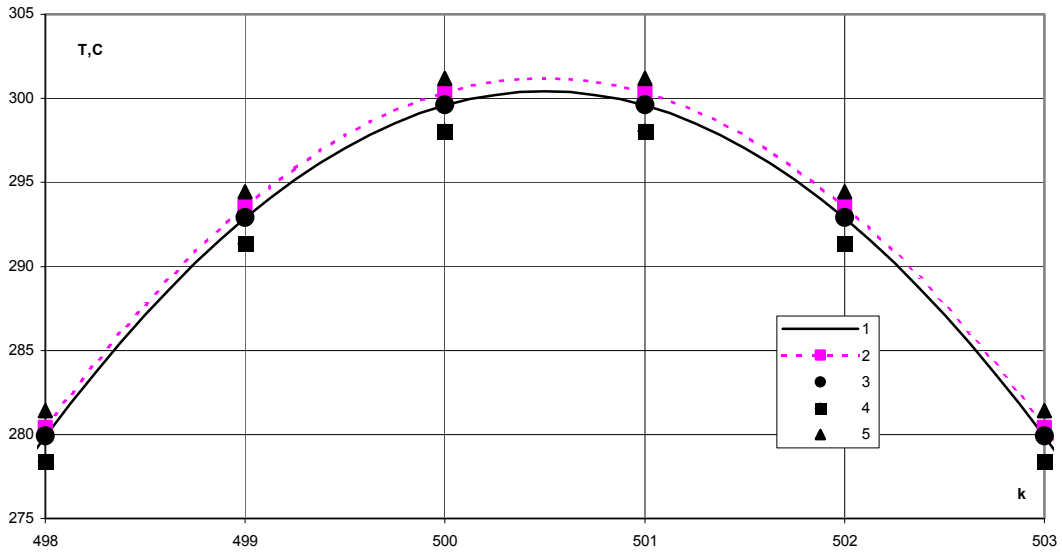

Fig. 8. The refined solution and error bounds in comparison with finite-difference and analytical solution. Zone A (Fig. 7). 1- analytical, 2-numerical 3- refined, 4- lower bound, 5 upper bound

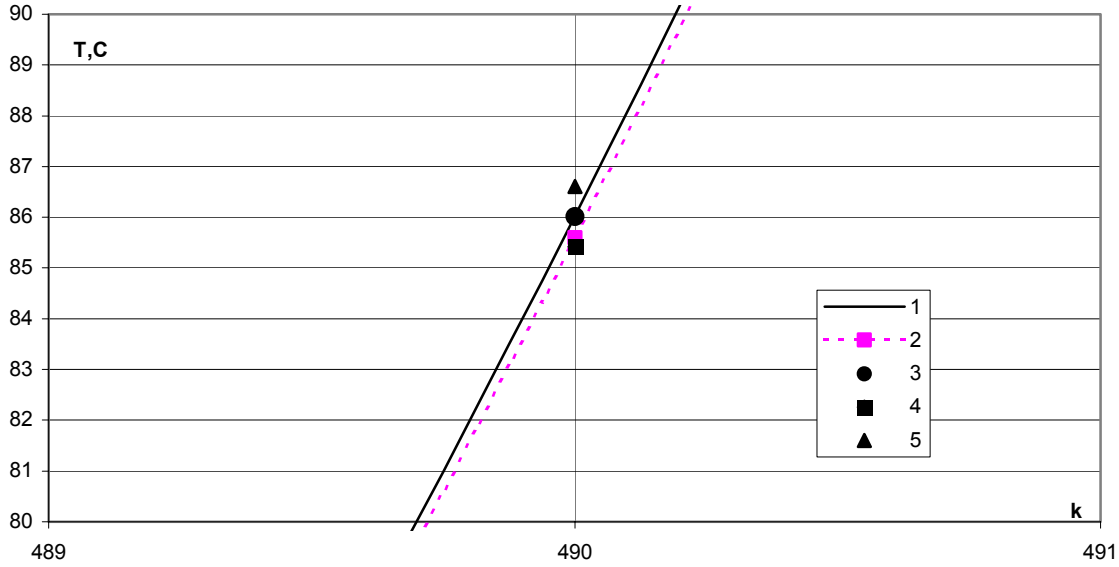

Fig. 9. The refined solution and error bounds in comparison with finite-difference and analytical solution. Zone B (Fig 7). 1- analytical, 2-numerical, 3- refined solution, 4-lower bound, 5- upper bound

Influence of discontinuities

A calculation of ΔT_x^{corr} and $\Delta T_x^{\sup}$ requires bounded high order derivatives. These are not always available, nevertheless (as was already demonstrated), the limitations on the smoothness requirements may be slightly relaxed. If the corresponding derivatives of the exact solution have jump discontinuities, the integral estimates exist, but asymptotically

reveal another (smaller) order of convergence. So, the thermal conductivity breaks (engendering discontinuities of temperature gradient) are a potential source of errors, which may be significantly greater than the nominal error of the finite-difference scheme. Herein we focus our attention on the discontinuities of primal parameters. The adjoint parameters are not differentiated, so are not so dangerous for our calculations. Some information on discontinuities of primal and adjoint parameters in related problems may be found in [18,11,13].

Let's study in numerical tests the asymptotic dependence of the error on the space step size for a temperature gradient discontinuity. In order to manage the discontinuity we used a divergent integro-interpolation method [32] assuming the following form:

First step

$$C_k \rho_k \frac{T_k^{n+1/2} - T_k^n}{\tau} = Z_{k+1/2}\left(T_k^n - T_{k+1}^n\right) + Z_{k-1/2}\left(T_k^n - T_{k-1}^n\right), \qquad (40a)$$

Second step

$$C_k \rho_k \frac{T_k^{n+1} - T_k^{n+1/2}}{\tau} = Z_{k+1/2}\left(T_k^{n+1} - T_{k+1}^{n+1}\right) + Z_{k-1/2}\left(T_k^{n+1} - T_{k-1}^{n+1}\right), \qquad (40b)$$

where $Z_{k+1/2} = \dfrac{2}{h_k\left(\dfrac{h_k}{\lambda_k} + \dfrac{h_{k+1}}{\lambda_{k+1}}\right)}$; $Z_{k-1/2} = \dfrac{2}{h_k\left(\dfrac{h_k}{\lambda_k} + \dfrac{h_{k-1}}{\lambda_{k-1}}\right)}$.

Corresponding estimates of the form (33) and (34) may be easily deduced but are very bulky and are not presented here. They may be found in [3].

Table 3 presents temperature error estimates (for central point at the final moment) depending on the spatial step for the thermal conductivity coefficient having a 10% jump at the center of the grid.

Table 3. Temperature error estimates depending the spatial step

h, m	ΔT_x^{corr}	$\Delta T_{x,1}^{\sup}$	$\Delta T_{x,2}^{\sup}$	$\Delta T_{x,3}^{\sup}$	$\Delta T_{x,4}^{\sup}$
0.0016	$4.6 \cdot 10^{-1}$	2.7	2.45	$6.9*10^{-1}$	$1.6*10^{-1}$
0.0008	$3.02*10^{-1}$	$8.61*10^{-1}$	$5.59*10^{-1}$	$1.28*10^{-1}$	$2.48*10^{-2}$
0.0004	$9.39*10^{-2}$	$4.1*10^{-1}$	$3.89*10^{-1}$	$1.19*10^{-1}$	$2.918*10^{-2}$
0.0002	$2.77*10^{-2}$	$3.57*10^{-1}$	$4.13*10^{-1}$	$1.32*10^{-1}$	$3.26*10^{-2}$
0.0001	$7.32*10^{-3}$	$2.24*10^{-1}$	$2.63*10^{-1}$	$8.58*10^{-2}$	$2.09*10^{-2}$
0.00005	$1.84*10^{-3}$	$1.2*10^{-1}$	$1.42*10^{-1}$	$4.65*10^{-2}$	$1.132*10^{-2}$

The data of Table 3 demonstrates that ΔT_x^{corr} has a convergence order similar to the smooth case (Table 2), while $\Delta T_{x,s}^{\sup}$ has a low order (not higher than unity) and decreases relatively slowly when the number of terms increases. This difference in behavior is caused by the compensation of the error before and past the break in the expression for ΔT_x^{corr} (33). Similar effects are well known in CFD ([20], for example). Corresponding expressions for $\Delta T_{x,s}^{\sup}$ contain moduli, so a compensation of the error before and past the discontinuity is impossible.

As another test we consider the evolution of the initial temperature distribution of a step shape. The initial, the final distribution of temperature and the location of estimated points are presented in Fig 10. The break of thermal conductivity is located at center point $(x_s = X/2)$ and coincides with a jump of the initial temperature.

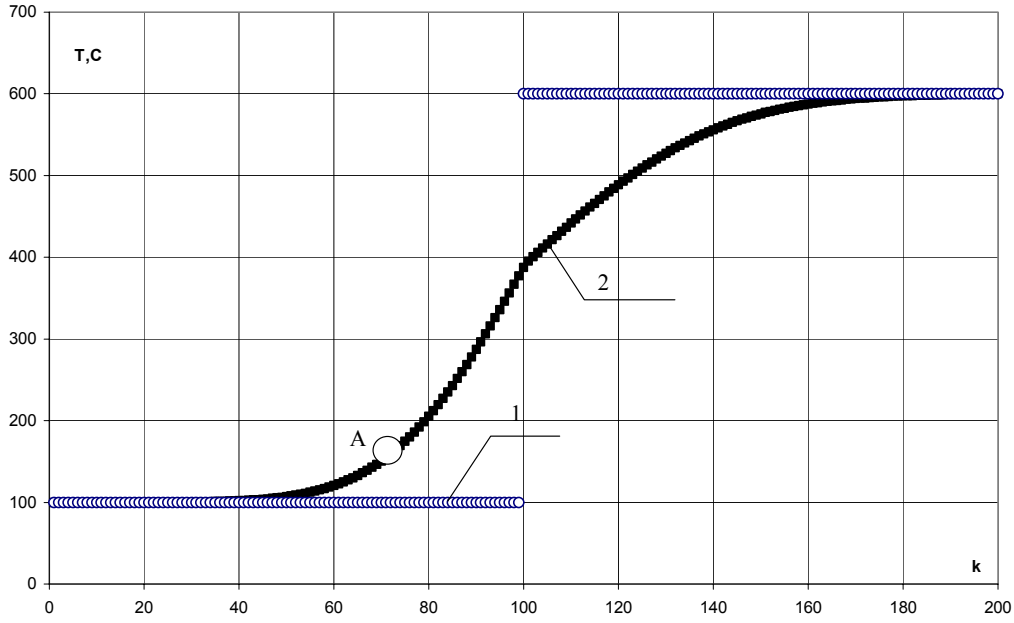

Fig. 10. Initial and final temperature distribution. 1- Initial temperature, 2- Final temperature, A- zone of estimation

In the left part, the initial temperature is denoted as T_{01}, thermophysical parameters are marked by index 1, correspondingly. In the right part the initial temperature is marked as T_{02}, while thermophysical parameters are marked by index 2, and the value of thermal conductivity is doubled comparing the left part. The thermal conductivity break causes the discontinuity in the temperature derivative that is of special interest here.

The corresponding analytical unsteady solution is described by expressions

$$\frac{T_{an}(t,x)-T_{01}}{T_{02}-T_{01}}=\frac{\theta}{1+\theta}\left(1-erf\left(-U_1\right)\right),\ x<x_s \qquad (41)$$

$$\frac{T_{an}(t,x)-T_{01}}{T_{02}-T_{01}}=\frac{\theta}{1+\theta}\left(1+\frac{erf\left(U_2\right)}{\theta}\right),\ x>x_s \qquad (42)$$

$$\theta = \left(\frac{\lambda_2 C_2 \rho_2}{\lambda_1 C_1 \rho_1} \right)^{0.5}, \; U_i = \frac{x - x_s}{2\sqrt{\lambda_i /(C_i \rho_i) t}}, \; erf(U_i) = \frac{2}{\sqrt{\pi}} \int_0^{U_i} e^{-u^2} du \qquad (43)$$

The deviation of finite-difference calculation from the analytical value and the estimates of errors are presented in Table 4.

Table 4. Estimates of temperature error in dependence on spatial step.

h, m	$T - T_{an}$	ΔT_x^{corr}	$\Delta T_{x,1}^{\sup}$	$\Delta T_{x,2}^{\sup}$	$\Delta T_{x,3}^{\sup}$	$\Delta T_{x,4}^{\sup}$
0.0016	$-4.0 \cdot 10^{-1}$	$-3.7 \cdot 10^{-1}$	$8.9*10^{-1}$	1.15	$3.7*10^{-1}$	$9.2*10^{-2}$
0.0008	$-1.55*10^{-1}$	$-1.4*10^{-1}$	$5.5*10^{-1}$	$6.6*10^{-1}$	$2.13*10^{-1}$	$5.3*10^{-2}$
0.0004	$-5.0*10^{-2}$	$-5.3*10^{-2}$	$3.6*10^{-1}$	$4.3*10^{-1}$	$1.4*10^{-1}$	$3.4*10^{-2}$
0.0002	$-1.2*10^{-2}$	$-2.0*10^{-2}$	$2.7*10^{-1}$	$3.3*10^{-1}$	$1.02*10^{-1}$	$2.6*10^{-2}$

The rate of convergence of $T - T_{an}$ and ΔT_x^{corr} is close to second order despite the influence of discontinuity. This is caused by mutual compensation of error in the vicinity of discontinuity as confirmed by an analysis of local distribution of error density $-\frac{\lambda}{12} h_k^3 \frac{\partial^4 T(t_n, x_k)}{\partial x^4} \Psi_k^n \tau$ (engendering ΔT_x^{corr} in accordance with (33)). The order of $\Delta T_{x,s}^{\sup}$ is close to unity (slightly below), which corresponds to the expected influence of the temperature gradient discontinuity. Calculations demonstrate the upper bound of error $\Delta T_{x,1}^{\sup}$ to be quite reliable, hence computation of the next terms is rendered unnecessary.

Thus, refining of the finite-difference solution and calculation of error bound using adjoint temperature may also be performed in presence of discontinuities in the temperature gradient.

Discussion. Formally, if we have an exact adjoint temperature we may obtain an arbitrarily small pointwise error. The approach is limited by the need to use temperature derivatives of high order that may be unbounded. In the first test problem, we used initial data $f_k = T_0(x_k)$ that are calculated analytically (35). The problem (1) with these initial data (on infinite interval) provides the existence of an infinite number of temporal and spatial derivatives. Here we use finite spatial interval X and boundary conditions (2), so the discontinuities on the boundaries are inevitable. Nevertheless, for the time duration considered the adjoint temperature is close to zero near the boundary. This provides applicability of estimates that use high order derivatives.

On the solution, having m bounded derivatives, we can obtain a correction and upper bound for the finite-difference approximation of the $p-th$ derivative under condition $m - p \geq 0$. Nevertheless, for small smoothness of solution $(m = p)$ refining does not increase the convergence rate (correcting and upper bound terms have the same order). Even past refining, the error will contain a component of the first order, and the upper bound (28) may contain an indefinite number of terms and may be too great. For smoother solution $(m - p \geq 1)$, it is feasible to raise the minimal convergence order by unity and obtain an upper bound of error using a single term of following order. And only for a smooth enough solution ($m \geq j + p + 1$, j-approximation order) is it feasible to raise the nominal order of scheme accuracy and obtain upper bounds of next order of accuracy.

As demonstrated by the numerical tests, the first upper bound estimate is reliable enough for smooth solutions because the next terms are significantly smaller. As the mesh size diminishes, this demonstrates a convergence rate higher by unit than the order of the finite difference scheme. Numerical tests demonstrated the upper bound to be not larger than required for its applicability in practice. Even under the presence of discontinuities in the temperature gradients, computations demonstrated feasibility of obtaining realistic upper

bounds despite a reduction of the convergence order.

Naturally, the present approach enables us to compute not only the error of temperature (written in the form of functional (5)) but also the error of other functionals of temperature. The differences are only in the form of the source in the adjoint equation (13). Under certain conditions mollification may be necessary for approximation of this source [23].

Conclusion. The pointwise error of temperature finite-difference computation may be reduced using adjoint equation. The upper bound of the remaining error may be obtained as a function of the sizes of temporal and spatial steps.

The computer time required for the pointwise temperature refining and the upper bound calculation is equal to the time required for temperature computation on the same grid.

***Nomenclature*:** *C*-thermal capacity; *h*- spatial step; *L*-Lagrangian**,** N_t-number of time steps; N_x – number of spatial nodes; *t*-time; t_f-duration of process; *T*-temperature; T_0- initial temperature; *x*-coordinate; *X*-thickness;

α, β, γ - coefficients in Taylor-Lagrange series, δ -Dirac's delta function; δT -Taylor series; ΔT – temperature variation; ΔT_x^{corr} -correctable error, connected with the expansion in space; ΔT_t^{corr} - correctable error, connected with the expansion in time; $\Delta T_{x,s}^{\sup}$ - component of bound of inherent error, connected with the expansion in coordinate; $\Delta T_{t,s}^{\sup}$ - component of bound of inherent error, related to the expansion in time; ε -functional; λ- thermal conductivity; ρ -density; τ -temporal step; Ω- domain *of* calculation; Ψ- adjoint temperature.

Indexes: *an*- analytical solution; *corr*- corrected error; *est* – estimated point; *exact*- exact solution; *k*-number of spatial mesh node; n-number of temporal step; *sup*- bound of inherent error; x-component of truncation error connected with Taylor expansion in coordinate; *t*- component of truncation error connected with Taylor expansion in time.

Acknowledgements

The second author acknowledges the support from the NSF grant number ATM-9731472 managed by Dr. Linda Peng whom he would like to thank for her support.

References

1. *M. Ainsworth and J. Tinsley Oden*, A Posteriori Error Estimation in Finite Element Analysis. (Wiley - Interscience, NY, 2000).
2. *A. Alekseev and I. M. Navon,* On Estimation of Temperature Uncertainty Using the Second Order Adjoint Problem//Int. Journal of Comput. Fluid Dynamics, Vol. 16 (2) (2002) 113–117.
3. *A. Alekseev*, Control of error of the finite difference solution of heat transfer equation using adjoint equation, Journal of Eng. Physics and Thermophysics, т. 77, N 1 (2004) (accepted).
4. *O.M. Alifanov Artyukhin E.A. and Rumyantsev S.V.,* Extreme Methods for Solving Ill-Posed Problems with Applications to Inverse Heat Transfer Problems, (Begell House Inc. Publ, 1996).
5. *M. H.Carpenter and J. H. Casper,* Accuracy of Shock Capturing in Two spatial Dimensions, - AIAA J, v. 37, N 9 (1999) 1072-1079.
6. *G. Efraimsson and G. Kreiss,* A Remark on Numerical errors Downstream of Slightly Viscous Shocks, SIAM J. of Numerical Analysis, Vol. 36, N 3 (1999) 853-863.
7. *B. Engquist and B. Sjogreen.* The Convergence Rate of finite Difference Schemes in the Presence of Shocks. SIAM Journal of Numerical Analysis 35 (1998) 2464 –2485.
8. *Lars Ferm and Per Lötstedt*, Adaptive error control for steady state solutions of inviscid flow, *SIAM J. Sci. Comput.* 23 (2002) 1777-1798.
9. *M. B. Giles,* On adjoint equations for error analysis and optimal grid adaptation in CFD//in *Computing the Future II: Advances and Prospects in Computational Aerodynamic*s, edited by M. Hafez and D. A. Caughey (Wiley, New York, 1998).
10. *M. B. Giles and E. Suli,* Adjoint methods for PDEs: a posteriori error analysis and postprocessing by duality, Acta Numerica, 11 (2002) 145-206.
11. *M. B. Giles* Discrete adjoint approximations with shocks. *Hyperbolic Problems: Theory, Numerics, Applications*, editors T. Hou and E. Tadmor (Springer-Verlag 2003).
12. *M. B. Giles and Pierce, N.A.,* Improved Lift and Drag Estimates Using Adjoint Euler Equations" Technical Report 99-3293, (AIAA, Reno, NV, 1999).
13. *M.B. Giles, M.C. Duta, J.-D. Muller and N.A. Pierce*.Algorithm developments for discrete

adjoint methods. *AIAA Journal*, 41(2) (2003) 198-205.

14. *R. Hartmann and P. Houston.* Goal-Oriented A Posteriori Error Estimation for Compressible Fluid Flows. *Numerical Mathematics and Advanced Applications*, Eds. F. Brezzi, A. Buffa, S. Corsaro and A. Murli, (Springer-Verlag, 2003) 775-784.
15. *R. Hartmann and P. Houston.* Goal-Oriented A Posteriori Error Estimation for Multiple Target Functionals, In T.Y. Hou and E. Tadmor, editors, *Hyperbolic Problems: Theory, Numerics, Applications*, , (Springer-Verlag, 2003) , 579-588.
16. *J. Hoffman and C. Johnson*, Computability and adaptivity in CFD*,* to appear as a chapter in (Encyclopedia of Computational Mechanics, Edited by E. Stein, R. de Borst and T.J.R. Hughes, 2003).
17. *J. Hoffman,* Adaptive finite element methods for LES: Duality based a posteriori error estimation in various norms and linear functionals (2002) *submitted to SIAM J. of Sci. Comp.*
18. *Chris Homescu and I. M. Navon* Optimal control of flow with discontinuities . *Journal of Computational Physics,* **Vol. 187 (** 2003) 660-682.
19. *C. Johnson,* , On Computability and Error Control in CFD. International J. for Numerical Methods in Fluids, Vol. 20 (1995) 777-788.
20. *Gunilla Kreiss, Gunilla Efraimsson, and Jan Nordstrom.* Elimination of First Order Errors in Shock Calculations. *SIAM Journal of Numerical Analysis*, 38(6) (2001) 1986–1998.
21. *G. I . Marchuk and V. V. Shaidurov,* Difference methods and their extrapolations, (Springer, N.Y., 1983).
22. *G. I. Marchuk,* Adjoint Equations and Analysis of Complex Systems**, (**Kluwer Academic Publishers, Dordrecht, 1995).
23. *J.T. Oden and S. Prudhomme,* Goal-Oriented Error Estimation and Adaptivity for the Finite Element Method, Computers&Mathematics with Applic. 41 (2001) 735-756.
24. *J. T. Oden and S. Prudhomme,* Estimation of modeling error in computational mechanics, *Journal of Computational Physics*, vol. 182 (2002) 496-515.
25. *M. A. Park,* Three–Dimensional Turbulent RANS Adjoint–Based Error Correction, AIAA Paper 2003-3849 (2003) 1-14.

26. *M. A. Park,* "Adjoint–Based, Three–Dimensional Error Prediction and Grid Adaptation," AIAA Paper 2002–3286 (2002) .

27. *N. A. Pierce and M. B. Giles*, Adjoint recovery of superconvergent functionals from PDE approximations *SIAM Re*v. 42 (2000) 247 - 264 .

28. *S. Prudhomme and J. T. Oden,* On goal-oriented error estimation for elliptic problems: Application to the control of pointwise errors, *Computer Methods in Applied Mechanics and Engineering*, vol. 176 (1999) 313-331.

29. *P. J. Roache,* "Quantification of Uncertainty in Computational Fluid Dynamics". Annual Review of Fluid Mechanics, 29 (1997) 123–160.

30. *C. J. Roy,* Grid Convergence Error Analysis for Mixed-Order Numerical Schemes. AIAA Journal., vol. 41, no. 4 (2003) 595 - 604.

31. *C. J. Roy, McWherter-Payne M.A., and Oberkampf, W. L.* "Verification and Validation for Laminar Hypersonic Flowfields", AIAA Paper 2000-2550, (2000).

32. *A . A. Samarskii,* Theory of difference schemes, (Marcel Dekker, NY, 2001).

33. D. A. Venditti and D. Darmofal, Grid Adaptation for Functional Outputs: Application to Two-Dimensional Inviscid Flow//J. Comput. Phys., 176 (2002) 40-69.

34. *D. A. Venditti and D. L. Darmofal,* Adjoint error estimation and grid adaptation for functional outputs: Application to quasi-one-dimensional flow, *J. Comput. Phys.* **16**4 (2000). 204 –227.

35. *Nail K. Yamaleev and Mark H. Carpenter,* On Accuracy of Adaptive Grid Methods for Captured Shocks, NASA/TM-2002-211415, (2002) 1-37.

36. Zhi Wang, Navon I. M., F.X. Le Dimet and X. Zou. The Second Order Adjoint Analysis: Theory and Applications, Meteorol. Atmos. Phys. v. 50 (1992) 3-20.

Figure Captions

Fig. 1. Initial and final temperature distribution. 1 - Initial temperature, 2- Final temperature.

Fig. 2. Temperature isolines

Fig. 3. Adjoint temperature isolines

Fig. 4. The comparison of numerical and analytical solutions in zone A (Fig. 1). 1- analytical, 2-numerical, 3-refined solution, 4- upper bound, 5- lower bound

Fig. 5. The comparison of numerical and analytical solutions in zone B. 1- analytical, 2-numerical, 3- refined solution, 4- upper bound, 5 lower bound

Fig. 6 The comparison of numerical and analytical solutions in zone C. 1- analytical, 2-numerical, 3- refined solution, upper bound, 5- lower bound

Fig. 7. Initial and final temperature distribution. 1- Initial temperature, 2- Final temperature

Fig. 8. The refined solution and error bounds in comparison with finite-difference and analytical solution. Zone A (Fig. 7). 1- analytical, 2-numerical 3- refined solution, 4- lower bound, 5 upper bound

Fig. 9. The refined solution and error bounds in comparison with finite-difference and analytical solution. Zone B (Fig. 7). 1- analytical, 2-numerical, 3- refined solution, 4-lower bound, 5- upper bound

Fig. 10. Initial and final temperature distribution. 1- Initial temperature, 2- Final temperature, A- zone of estimation